Green Chemistry & Technology Letters
eISSN: 2455-3611, Vol 4, No 2, 2018, pp 01-09
https://doi.org/10.18510/gctl.2018.421

GREEN CHEMICAL SYNTHESIS AND PROPERTIES OF SOLID DISPERSIONS OF BENZIMIDAZOLE –B. NAPHTHOL BINARY DRUG SYSTEM

H. Shekhar and Manoj Kumar
Department of Chemistry, V.K.S. University, Ara-802301, India
Email: hshe2503@rediffmail.com, manojcbpstk@gmail.com,

Article History: Received on 13th May, Revised 25th August, Published on 29th September 2018

Abstract

With view to synthesize and characterize the enhanced pharmaceutical properties of the solid-liquid dispersions of binary drug system through green chemical technique the present communication have been undertaken for detailed investigation of thermodynamic and interfacial properties of benzimidazole (BI) and β. naphthol (βN) binary eutectic and non-eutectic drug dispersions. Eutectic solid dispersion was observed at 0.657 mole fraction of β. naphthol (βN) and at melting temperature 90°C.

Thermodynamic quantities; Partial and Integral excess Gibbs energy (g^E), excess enthalpy (h^E), excess entropy (s^E) of eutectic and non-eutectic dispersions were determined with the help of activity coefficient data. The negative deviation from ideal behavior has been seen in the system which refers stronger association between unlike molecules during formation of binary mix. The negative value of Gibbs free energy of mixing (ΔG^M) refers the mixing for all eutectic and non-eutectic dispersions is spontaneous. The solid-liquid interfacial characteristics i.e., entropy of fusion per unit volume (ΔS_V), solid-liquid interfacial energy (σ), roughness parameter (α), grain boundary energy and roughness parameter (α) of eutectic and non-eutectic solid dispersions have been reported.

The size of critical nucleus at different undercoolings has been found in nanoscale, which may be a big significance in pharmaceutical world. The value of roughness parameter, $\alpha > 2$ was observed which manifests the faceted and irregular growth leads in the system.

Keywords*: SLE, Mixing and excess thermodynamic functions, thermal stability, Interfacial energy, Driving force of nucleation, Critical radius.*

INTRODUCTION

Benzimidazols have been reported to have diverse pharmaceutical and biological activities. The compounds bearing imidazolyl moiety possess a wide spectrum of biological activities which is related to their capacity to transfer electrons to scavenge reactive oxygen species. B.naphthol nucleus is an biologically important ties in the vitamin B_{12} which show diverse types of biological and pharmacological properties [1-6]. Several derivatives of benzimidazoles have been reported as antagonists, dopamine β-hydroxylase inhibitors and inhibitors for endothelial cell growth. Its derivatives have widely been reported as antimicrobial and anti-tumor agents. The chemistry and pharmacology of hetrocyclic benzimidazoles have been of very significant interest to medicinal chemistry because its new drugs designing a number of derivatives possess various biological and medicinal activities [7-9] such as antioxidant, anticonvulsant, antifungal, antiprotozoal, antiviral, anthelmintic, antihypertensive, antineoplastic, anti-inflammatory, analgesic, anti-hepatitis B virus and antiulcer activity. The optimization of benzimidazole based structures has got better result in various drugs available in the market, as mebendazole (Anthelmintic), pimobendan (Ionodilator), and omeprazole (Proton pump inhibitor). In it benzene ring is fused to the 4 and 5 positions of an imidazole ring. Benzimidazole is also 1, 3-benzodiazoles. These days researches on the solid dispersion of binary drug systems have been gaining credit and used as model system for studying the rapid growth and vast pharmacological nano particles drugs which are very important parameters in controlling the final physical , chemical and medicinal properties of solid dispersion. Further study on binary drug dispersions to a great extent can be done with the help of kinetic, themodynamic and interfacial investigation. For that detailed investigations of β-naphthol (βN) and benzimidazole (BI) binary eutectic and non-eutectic drug dispersions have been mentioned in this research article. β-naphthol have gained much significant importance in the area of pharmaceutical applications. Some of the derivatives of β-naphthol have been highlighted as anticancer, antimicrobial and anti-tumor agents. The scientific and medicinal worth of BI recognized as multidrug-resistant mycrobacterium, Methicillin-resistant staphytococus aureus, tuberculosis, and plasmid-antibiotic-resistant genes which are responsible for the major global lethal and noscomial infections and death of over 4 million people per year. The mild neuroleptic action of BI has got bigger credit comparatively similar equivalents compounds for the management of these infections. It also inhibits micro-organisms causes for antibiotic resistance [10] and calcium binding to calmodulion type proteins of the calcium channel verapamil.

Due to distinguished biological and pharmacological importants of β-naphthol and benzimidazoles, may take a good lead in developing and designing of new binary drugs. However, very little information has been reported on the binary drug solid dispersion materials. In recent pasts pharmaceutical properties of some binary drug dispersion has been emphasizing on the solubility, dissolution rate, hygroscopicity and chemical stability. Keeping in view of better pharmacological performance and efficacy of binary product, it is aimed to synthesize the benzimidazole (BI) and β-naphthol (βN) binary drug dispersions

in the solid state using green chemical process without aid of solvent and to emphasize thermodynamic and investigation such as phase diagram, thermodynamic excess and mixing functions, thermal stability, interfacial energy, driving force of solidification and surface roughness.

EXPERIMENTAL DETAILS

β-naphthol (βN) (BDH, India) and Benzimidazoles (BI) (Sigma, India) were used for investigation. The melting point of β-naphthol and Benzimidazoles was found 124°C and 170°C respectively. For measuring the phase diagram of βN -BI system, mixtures of different compositions of both were taken in glass test tubes and prepared samples by repeated heating and followed by chilling in ice. The melting temperatures of solid dispersions were determined by the thaw-melt method [11]. The melting and thaw temperatures were determined using Toshniwal melting point apparatus fitted with a precision thermometer. The value of enthalpy of fusion of β-naphthol and Benzimidazoles was determined by using Stanton Redcroft STA-780 series unit [12].

RESULTS AND DISCUSSION

SLE Study

The solid liquid equilibrium (SLE) digram of βN -BI system reported in Table 1 and in fig.1 shows the formation of an eutectic (E) and non-eutectics solid dispersions (A1-A9). The temperature of βN (124°C) decreases on the addition of BI (M.P., 170°C) and moves down minimum and further increases. Eutectic E (0.343 mole fraction of BI) is obtained at 90°C. At the eutectic temperature a liquid phase L and two solid phases (S_1 and S_2) exists in equilibrium and the system becomes invariant. Homogenous binary liquid exists in the region above the eutectic temperature and two solid phases got the region below the eutectic temperature.

Thermodynamic Study

The values of heats of fusion of eutectic and non-eutectic solid dispersions are calculated using the mixture law. The value of heat of fusion of binary eutectic and non-eutectic solid dispersions A_1-A_8 and E is mentioned in Table 1. The activity coefficient and activity of components for in the present system has been evaluated from the equation [13] given below

$$-\ln\chi_i\gamma_i = \frac{\Delta H_i}{R}\left(\frac{1}{T_e} - \frac{1}{T_i}\right) \quad (1)$$

where χ_i, *and* γ_i are mole fraction and activity coefficient of the component *i* in the liquid phase respectively. ΔH_i is the heat of fusion of component i at its melting point T_i, T_e is the melting temperature of solid dispersions and R is the gas constant. The value of activity and activity coefficient of the components in the binary product, are very helpful to evaluate mixing and excess thermodynamic functions.

Mixing Functions

For illustrating the mixing characteristics of components in the binary system Integral molar free energy of mixing, (ΔG^M), molar enthalpy of mixing ΔH^M) and molar entropy of mixing (ΔS^M) and partial molar free energy of mixing ($G^-_i{}^M$) of the binary solid dispersions were determined by the following equations

$$\Delta G^M = RT\,(\chi_{BI}\ln a_{BI} + \chi_{\beta N}\ln a_{\beta N}) \quad (2)$$

$$\Delta S^M = -R\,(\chi_{BI}\ln\chi_{BI} + \chi_{\beta N}\ln\chi_{\beta N}) \quad (3)$$

$$\Delta H^M = RT\,(\chi_{BI}\ln\Delta_{BI} + \chi_{\beta N}\ln\Delta_{\beta N}) \quad (4)$$

$$G^-_i{}^M = \mu^-_i{}^M = RT\ln a_i \quad (5)$$

where $G^-_i{}^M$ ($\mu^-_i{}^M$) is mixing chemical potential of component$_i$ in binary mix. Δ_i and a_i are the activity coefficient and activity of component respectively. The negative value [14] of molar free energy of mixing of solid dispersions mentioned in Table 2 confirms the mixing in all cases is spontaneous. The integral molar enthalpy of mixing value corresponds to the value of excess integral molar free energy of the system favors the regular behavior of the binary solutions.

Excess Functions

The nature of the interactions between the components of binary eutectic and non-eutectic Products is highlighted on the basis of values of the excess thermodynamic functions such as integral excess integral free energy (g^E), excess integral entropy (s^E) and excess integral enthalpy (h^E) which were calculated as below

$$g^E = RT(\chi_{BI} \ln \gamma_{BI} + \chi_{\beta N} \ln \gamma_{\beta N}) \quad (6)$$

$$s^E = -R\left((\chi_{BI} \ln \gamma_{BI} + \chi_{\beta N} \ln \gamma_{\beta N} + \chi_{BI} T \frac{\delta \ln \gamma_{BI}}{\delta T} + \chi_{\beta N} T \frac{\delta \ln \gamma_{\beta N}}{\delta T} \right) \quad (7)$$

$$h^E = -RT^2\left(\chi_{BI} \frac{\delta \ln \gamma_{BI}}{\delta T} + \chi_{\beta N} \frac{\delta \ln \gamma_{\beta N}}{\delta T} \right) \quad (8)$$

The excess chemical potential μ_i^{-M} or excess partial free energy of mixing g_i^{-E} is defined as

$$g_i^{-E} = \mu_i^{-M} = RT \ln \gamma_i \quad (9)$$

The values of $\Delta \ln \Delta_i / \Delta T$ can be determined by the slope of liquidus curve near the alloys. The values of the excess thermodynamic functions are reported in Table 3. The value of the excess free energy is a measure of the departure of the system from ideal behavior. The reported excess thermodynamic data favor the previous report of plausible interaction between the parent components during the formation of mix. The negative g^E value [15] for eutectic and A3, A4, A5, A6 non-eutectic solid dispersions leads the ground of stronger interaction between unlike molecule s in binary mix. The positive g^E value for A1,A2 and A7-A9 favors the interaction of stronger association between like molecules of binary product. The excess entropy gain in the system is due to the change in configurational energy and non continuity in potential energy which indicates an increase in randomness in the system.

Gibbs-Duhem Equation

The partial molar quantity, activity and activity coefficient are very helpful to derive Gibbs-Duhem equation [16]

$$\sum \chi_i dz_i^{-M} = 0 \quad (10)$$

$$or \ \chi_{BI} dH_{BI}^{-M} + \chi_{\beta N} dH_{\beta N}^{-M} = 0 \quad (11)$$

$$or \ dH_{BI}^{-M} = \frac{\chi_{\beta N}}{\chi_{BI}} dH_{\beta N}^{-M} \quad (12)$$

$$or \ [H_{BI}^{-M}]_{x_{BI}=y} = \int_{\chi_{BI}=y}^{\chi_{BI}=1} \frac{\chi_{\beta N}}{\chi_{BI}} dH_{\beta N}^{-M} \quad (13)$$

A graph plotted using equation (13) between $H_{\beta N}^{-M}$ and $\chi_{\beta N}/\chi_{BI}$ measures the solution of the partial molar heat of mixing of a constituent βN in binary mix and plot determine between $\chi_{\beta N}/\chi_{BI}$ and $\ln a_\beta \Delta$ determines the value of activity of component βN in binary mix.

Stability Function

For elucidating thermodynamic stabilizing behavior of binary product, thermodynamic stability and excess stability functions has been determined by the second derivative of their molar free energy and excess energy respectively, with respect to the mole fraction of either constituent:

$$\text{Stability} = \frac{\partial^2 \Delta G^M}{\partial x^2} = -2RT \frac{\partial \ln a}{\partial (1-x)^2} \quad (14)$$

$$\text{Excess Stability} = \frac{\partial^2 g^E}{\partial x^2} = -2RT \frac{\partial \ln \gamma}{\partial (1-x)^2} \quad (15)$$

The value of stability and excess stability were calculated by multiplying the slope of lna vs $(1-x)^2$ and lnγ vs $(1-x)^2$ plots with -2RT. The best polynomial equation of the curve generated is given as:

$$\ln \gamma = 3.68(1-x)^2 - 21.44(1-x)^4 + 81.99(1-x)^6 - 146.84(1-x)^8 + 126.(1-x)^{10} - 41.47(1-x)^{12} \quad (16)$$

The slope of the curve (figure) obtained by differentiating the above equation with respect to $(1- x)^2$ has been used to calculate the excess stability of the βN -BI system. The values of total stability to the ideal stability and defined as

$$\text{Ideal Stability} = \frac{RT}{x(1-x)} \qquad (16.1)$$

These values remark there is appreciable thermodynamic stability in the binary product. The fig.2 for the stability, excess stability and ideal stability in the form of composition and partial Gibb's energy favors the formation of the binary products and their mixing.

Interfacial Investigation

The Solid-Liquid Interfacial Energy (σ)

Previous report is evident for measurement of **σ** value which keeps a variation of 50-100% between experimentally observed and calculated value of interfacial energy 'σ', determined using the value of melting enthalpy change. It was found that there is a good agreement [17] of calculated value of the solid-liquid interfacial energy (σ) from melting enthalpy change and values obtained from experiment. Turnbull relationship [18] is related to interfacial energy and enthalpy change which was determined for binary solid dispersions using Turnbull equation.

$$\sigma = \frac{C\Delta H}{(N)^{1/3}(V_m)^{2/3}} \qquad (17)$$

The coefficient *C* tents between 0.33 to 0.35 for nonmetallic system, V_m and N are molar volume and Avogadro's constant respectively. The value of the solid-liquid interfacial energy of β. naphthol and benzimidazole was found to be 3.81 x 10^{-02} and 2.84 x 10^{-02} J m^{-2} respectively and σ value of the solid dispersions was given in Table 1.

Gibbs-Thomson Coefficient (τ)

The value of Gibbs-Thomson coefficient also measures value of σ based on equal thermal conductivities of solid and liquid phases for some transparent materials. It was calculated using Gibbs-Thomson equation for a planar grain boundary on planar solid-liquid interface of binary product and is expressed as

$$\tau = r\Delta T = \frac{TV_m\sigma}{\Delta H} = \frac{\sigma}{\Delta S_V} \qquad (18)$$

where r is the radius of grooves of interface, τ is the Gibbs-Thomson coefficient and ΔT is the dispersion in equilibrium temperature and similar type of results were determined by using the help of Hunt and Lu method [19] for the materials having known grain boundary shape, temperature gradient, and the ratio of thermal conductivity of the equilibrated liquid phases to solid phase ($R = K_L/K_S$).The Gibbs-Thomson coefficient for βN, BI and their solid dispersions are found in the range of 7.61 – 8.00 x 10^{-06} Km and is reported in Table 1.

Interfacial Grain Boundary Energy (σ_{gb})

The internal surface grain boundary is can be understood in a the best way to nucleation of materials on surfaces during liquid-solid transformation. A considerable force is employed at the grain boundary groove in anisotropic interface. Using a numerical method [20] the interfacial grain boundary energy (σ_{gb}) was determined without applying the temperature gradient for the grain boundary groove shape. The grain boundary energy can be obtained by the equation:

$$\sigma_{gb} = 2\sigma\cos\theta \qquad (19)$$

where θ is equilibrium contact angle precipitates at solid-liquid interface of grain boundary. In case zero contact angle the grain boundary energy could be twice the solid-liquid interfacial energy. The value of σ_{gb} for solid βN and BI was found to be 5.49 x 10^{-2} and 7.37 x 10^{-2}Jm^{-2} respectively and the value for all solid dispersions is given in Table 1.

The Effective Entropy Change (ΔS_v)

The effective entropy change **(ΔS_v)** and the volume fraction of phases in the binary dispersion are inter-linked and jointly to decide the interfacial morphology during solidification of materials. The entropy of fusion (ΔS = ΔH/T) value (Table 1) of solid dispersions is calculated by heat of fusion values of the materials because the volume fraction of the two phases depends on the ratio of effective entropy change of the phases. The effective entropy change per unit volume (ΔS_V) is given by

$$\Delta S_V = \frac{\Delta H}{T}.\frac{1}{V_m} \qquad (20)$$

Where V_m is the molar volume of solid phase and T is the melting temperature. The entropy of fusion per unit volume (ΔS_V) for βN and BI was found 373 and 477 kJK^{-1}m^{-3} respectively. Values of ΔS_V for all are reported in Table 1.

Green Chemistry & Technology Letters
eISSN: 2455-3611, Vol 4, No 2, 2018, pp 01-09
https://doi.org/10.18510/gctl.2018.421

The Driving Force of Nucleation (ΔG_v)

Gibb's free energy generated during growth of crystalline solid is due to change in enthalpy, entropy and specific volume. A metastable phase usually leads in a supersaturated or super-cooled liquid. The driving force of nucleation during liquid-solid transformation arises being a difference in Gibb's energy of the two phases. However various theories of solidification process were discussed taking a base of diffusion, kinetic and thermodynamic features. The lateral motion of rudementry steps in liquid brings forth stepwise with non-uniform surface at low driving force while continuous and uniform surface raises at sufficiently high driving force. The driving force of nucleation during solidification (ΔG_V) was determined at different undercoolings (ΔT) as follows [21]

$$\Delta G_V = \Delta S_v \Delta T \quad (21)$$

It is well known the surface free energy which resists ΔG_V increases due to creation of a new solid-liquid interface. Actually the solid phase in surrounding in super saturated liquids nucleates as small spherical cluster of radius arising due to random motion of atoms. The value of ΔG_V for each solid dispersions are shown in the Table 4.

The Critical Radius (r*)

During liquid-solid transformation embryos originate rapidly and dispersed around unsaturated liquid which on undercooling the liquid becomes super saturated and provides embryo of a critical size with radius r* for nucleation. It has been determined by the Chadwick relation [22]

$$r^* = \frac{2\sigma}{\Delta G_V} = \frac{2\sigma T}{\Delta H_V \Delta T} \quad (22)$$

where ΔH_V, σ are the enthalpy of fusion of the compound per unit volume and the interfacial energy respectively. The critical size of the nucleus for the components solid dispersions was evaluated at different undercoolings and values are mentioned in Table 5. It is evident from table that the critical nucleus size of materials decreases with increase in the undercooling of the melt. The existence of embryo and size of embryo can be imagined in the liquid at any temperature. The value of r* for pure components (βN and BI) and solid dispersions lies between 43.5 to 160 nm at undercooling 1– 3.5°C.

Critical Free Energy of Nucleation (ΔG*)

A localized activation or critical free energy of nucleation (ΔG*) generating critical nucleus is evaluated [23] as

$$\Delta G^* = \frac{16}{3} \frac{\pi \sigma^3}{\Delta G_v^2} \quad (23)$$

The value of ΔG* for binary products and pure components has been found in the range of 10^{-15} to 10^{-16} J per molecule at different undercoolings, and has been reported in Table 6.

Interface Morphology

The growth Morphology on the surfaces is highlighted on the combined ground of thermodynamics, kinetics, fluid dynamics, crystal structures and interfacial sciences. In past the solid-liquid interface morphology has been predicted in the light of the value of the entropy of fusion. The type of growth from a binary melt [24] depends upon a factor α, defined as:

$$\alpha = \xi \frac{\Delta H}{RT} = \xi \frac{\Delta S}{R} \quad (24)$$

where ΔS/R (Jackson's roughness parameter α) is the entropy of fusion (dimensionless), ξ is a crystallographic factor depending upon the geometry of the molecules and has a value less than or equal to one and R is the gas constant. The solid-liquid interface is atomically rough and exhibits non-faceted growth in the case of α value be less than two. The value of Jackson's roughness parameter (α) is reported in Table 1. For the entire eutectic and non- eutectic solid dispersions the α value was found greater than 2 indicating the faceted [25] growth leads in all the cases.

CONCLUSION

The solid-liquid equilibrium phase diagram of βN -BI system forms of simple eutectic solid dispersion. The thermodynamic mixing function, ΔG^M values for eutectic and non-eutectics are being found negative which favours spontaneous mixing in all the binary drugs. The negative value of g^E for eutectic and non-eutectic A3-A6 favours the stronger association between unlike molecules and positive g^E value for A1-A2 and A7-A9 suggests there is stronger association between like molecules.

ACKNOWLEDGEMENT

We are very thankful to the Head, Department of Chemistry, V K S University, Ara -802301, India for providing necessary research facilities.

REFERENCES

1. Arora Shefali. Study of Some Benzimidazole Compounds as Antibacterial and Antifungal Agents. J. Pharm. Sci. & Res. 3 (2011) 1310-1314.
2. Michele Tonelli, Matteo Simone, et al. Antiviral activity of benzimidazole derivatives. II. Antiviral activity of 2-phenylbenzimidazole derivatives. Bioorganic & Medicinal Chemistry 18 (2010) 2937-2953.
3. Ingle R. G. and Magar D. D. Heterocyclic Chemistry of Benzimidazoles and potential Activities of Derivatives. Int. J. Drug Res. Tech. 1 (2011) 26-32.
4. Chinnadurai Satheeshkumar[1], Mahalingam Ravivarma[1], et al., Synthesis, Antimicrobial and Molecular Docking studies of Benzimidazole and Benzotriazole based Dicationic Sulphonophanes. Canadian Chemical Transactions 2 (2014) 248-257.
5. Rajakumar P., Sekar K., Shanmugaiah V., Mathivanan N. Synthesis of some novel imidazole-based diactionic carbazolophanes as potential antibacterials. Bioorg. Med. Chem. Lett. 18 (2008) 4416-4419.
6. Boiani M., Gonzalez M. Imidazole and benzimidazole derivatives as chemotherapeutic agents. Mini-Rev. Med. Chem. 5 (2005) 409-424.
7. Zhang L., Peng X. M., Damu G. L. V., Geng R. X., Zhou C. H. Comprehensive Review in Current Developments of Imidazole-Based Medicinal Chemistry. Med. Res. Rev. (2013) 1-98.
8. Sharma M. C., Kohli D. V., Sharma Smita and Sharma A. D. Synthesis and antihypertensive activity of some new benzimidazole derivatives of 4'-(6-methoxy-2-substituted-benzimidazole-1-ylmethyl)- biphenyl-2-carboxylic acid in the presences of $BF_3.OEt_2$. Pelagia Research Library 1 (2010) 104-115.
9. S. Khokra L. & Choudhary Deepika. Benzimidazole an important Scaffold in drug Discovery. Asian Journal of Biochemical and Pharmaceutical Research 3 (2011).
10. Yu. L. & Reutzel-Edens S. M. Crystallization, Encyclopedia of Food Sciences and Nutrition (Second Ed.), Elsivier Science Ltd. Amsterdam (2003).
11. Shekhar H. and kumar Manoj. Thermodynamic and interfacial studies on solid dispersion of phenothiazine-2-methylimidazole drug system, Journal of Chemistry and Pharmaceutical Research, 7 (2015) 37-45.
12. Salim S. S., Ph. D. Thesis, Study of Multiphase Organic Materials, V. K. S. University, Ara, Bihar (2009).
13. Kant Vishnu and Shekhar H., Phase Behaviour, Molecular Interaction and Morphological Studies on Co-crystals of nicotinamide-p-Nitroaniline Drug System, International Journal of Pure and Applied Chemistry, 9 (2014) 127-137.
14. Shekhar H. and Salim S.S., Themodynamics of Organic Alloys: Mixing and Excess Function. J. Indian Chem. Soc. 91 (2014) 2189-2196.
15. Kumar Manoj and Shekhar H., Thermodynamic and Interfacial Investigation of Phenothiazine-Resorcinol Binary System. Internation Journal of Chemistry 4 (2015) 257-268.
16. Wisniak J. & Tamir A. Mixing and Excess Thermodynamic Properties (a literature source book), Phys. Sci. Data 1, Elsevier, New York (1978).
17. Singh, N. B. & Glicksman, M. E. Determination of the mean solid-liquid interface energy of pivalic acid. Journal Cryst Growth 98 (1989) 573-580.
18. Turnbull, D. Formation of Crystal nuclei in Liquid Metals. J. Chem. Phys. 21 (1950) 1022-1027.
19. Hunt J. D & Lu S. Z. 1994. Hand Book of Crystal Growth Ed. DTJ Hurle, Elsevier, Amsterdam, 112.
20. Shekhar H. & Kant Vishnu. Thermodynamics of Nicotinamide Based Binary Drug System, Lambert Academic publishing Germany (2013).
21. Gupta P., Agrawal T. Das S. S. & Singh N. B. Solvent Free Reactions, Reactions of Nitrophenols in 8-Hydroxyquinoline-Benzoic Acid Eutectic Melt, Journal of Thermal Analysis and Calorimetry 104 (2011) 1167-1176.
22. Chadwick G. A. Metallography of Phase Transformation, Butterworths, London 61 (1972).
23. Nieto R., Gonzalez M. C. and Herrero F. Thermodynamics of mixtures, Function of mixing and excess functions, American Journal of Physics 67 (1999) 1096-1099.
24. Hunt, J. D. & Jackson, K. A. Binary Eutectic Solidification. Trans Metall Soc AIME. 236 (1966) 843-852.
25. Bai Xian-Ming & Li Mo. Calculation of Solid-liquid interfacial free energy: A classical nucleation theory based approach, J. of Chem. Phy. 124 (2006) 124707-12.

Green Chemistry & Technology Letters
eISSN: 2455-3611, Vol 4, No 2, 2018, pp 01-09
https://doi.org/10.18510/gctl.2018.421

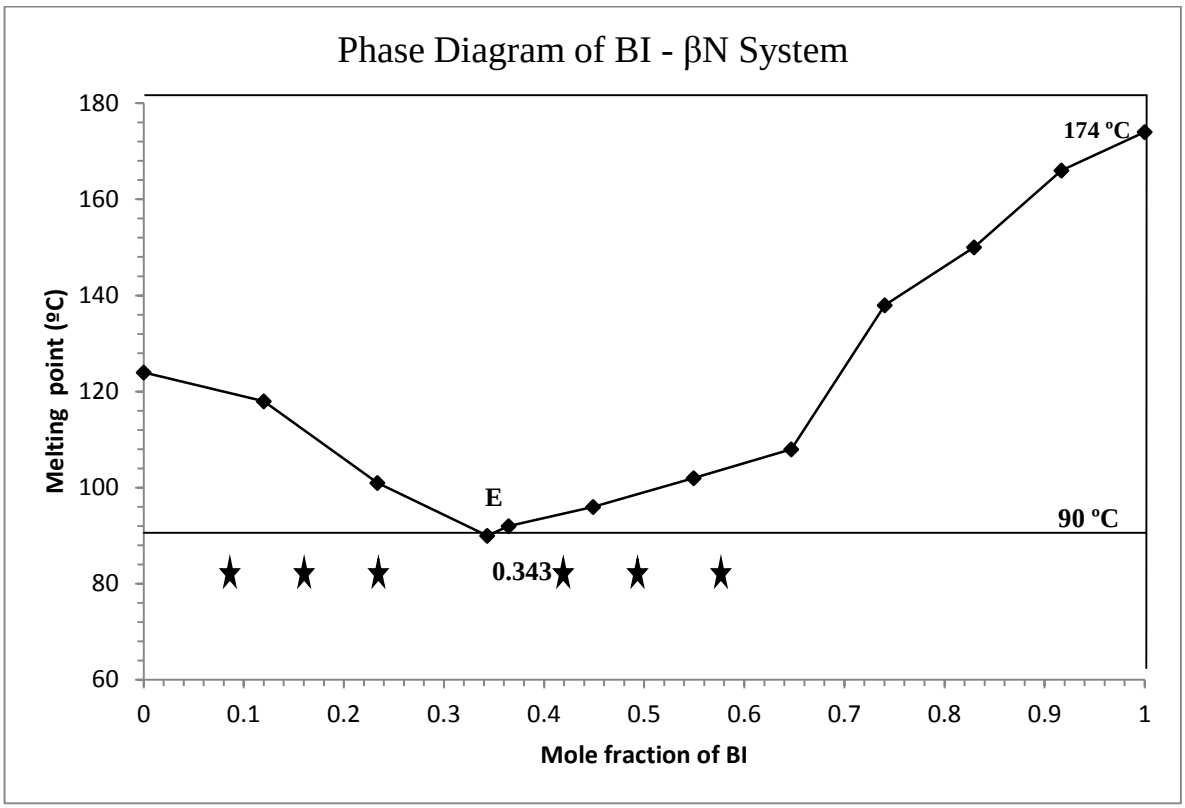

Fig. 1 Phase Diagram of BI - βN System

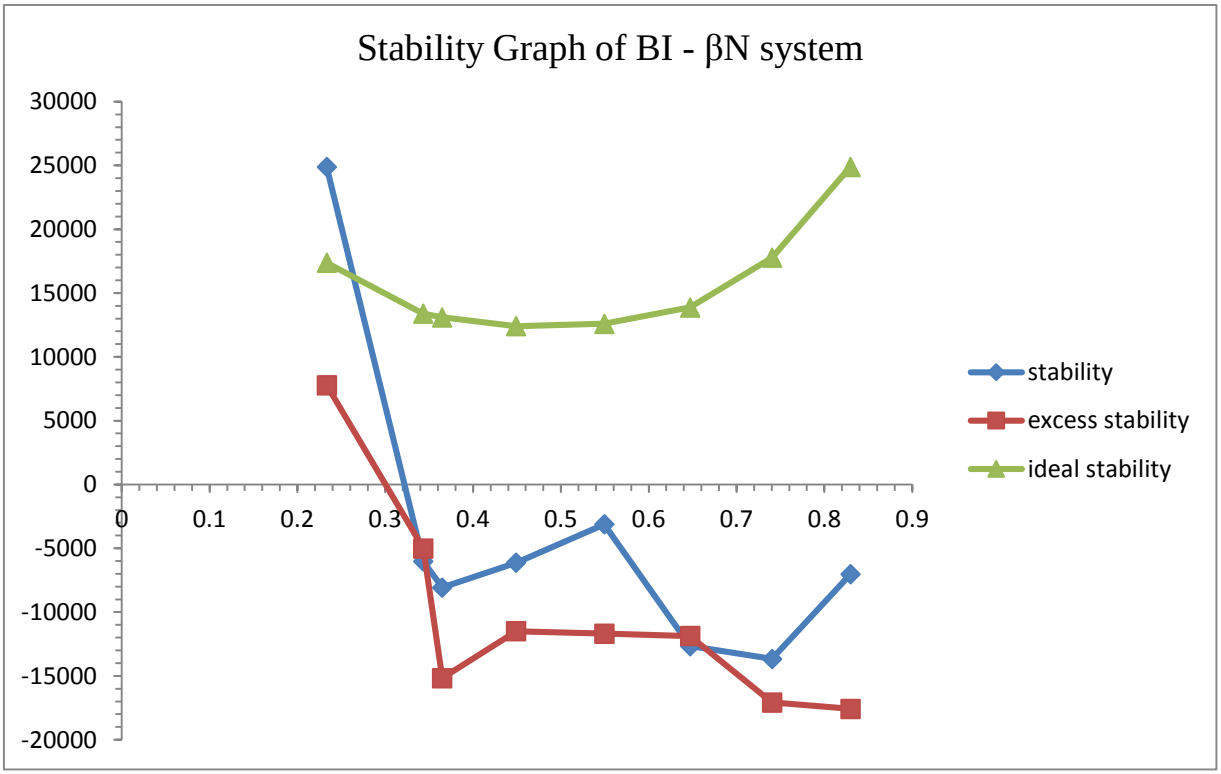

Fig. 2 Stability Graph of BI - βN system

Green Chemistry & Technology Letters
eISSN: 2455-3611, Vol 4, No 2, 2018, pp 01-09
https://doi.org/10.18510/gctl.2018.421

Table 1: Phase composition, melting temperature, heat of fusion(ΔH), values of entropy of fusion per unit volume (ΔS_v), interfacial energy(σ), grain boundary energy(Δ_{gb}), Gibbs-Thomson coefficient (τ) and roughness parameter(α)

Alloy	χ_{BI}	MP	ΔH (J/mol)	ΔS (J/mol/K)	α	$\sigma \times 10^2$ (J/m^2)	$\sigma_{gb} \times 10^2$ (J/m^2)	ΔS_v ($kJ/m^3/K$)	ΔH_v	$\tau \times 10^6$ Km
A1	0.120	118	17864.87	45.69	5.50	2.94	5.69	395.52	154.65	7.44
A2	0.233	101	18200.95	48.67	5.85	3.04	5.88	430.64	161.06	7.07
E	0.343	90	18525.99	51.04	6.14	3.14	6.07	461.53	167.54	6.81
A3	0.365	92	18589.77	50.93	6.13	3.16	6.11	462.58	168.84	6.84
A4	0.449	96	18839.07	51.05	6.14	3.24	6.26	471.68	174.05	6.87
A5	0.549	102	19136.08	51.03	6.14	3.34	6.45	481.33	180.50	6.94
A6	0.647	108	19425.50	50.99	6.13	3.44	6.64	490.93	187.04	7.00
A7	0.740	138	19701.35	47.94	5.77	3.53	6.82	470.90	193.54	7.50
A8	0.830	150	19965.79	47.20	5.68	3.63	7.00	472.87	200.02	7.67
A9	0.917	166	20224.23	46.07	5.54	3.72	7.19	470.64	206.61	7.91
BI		174	20470.00	45.79	5.51	3.81	7.37	476.78	213.12	8.00
βN		124	17510.00	44.11	5.31	2.84	5.49	373.23	148.17	7.61

Table 2: Value of partial and integral mixing of Gibbs free energy(ΔG^M), enthalpy(ΔH^M) and entropy(ΔS^M) of BI-βN system

Alloy	ΔG_{BI}^{-M} J/mol	$\Delta G_{\beta N}^{-M}$ J/mol	ΔG^M J/mol	ΔH_{BI}^{-M} J/mol	$\Delta H_{\beta N}^{-M}$ J/mol	ΔH^M J/mol	ΔS_{BI}^{-M} J/mol/K	$\Delta S_{\beta N}^{-M}$ J/mol/K	ΔS^M J/mol/K
A1	-2564.47	-264.63	-540.36	4331.00	150.52	651.72	17.64	1.06	3.05
A2	-3342.98	-1014.43	-1557.98	1180.86	-187.85	131.64	12.10	2.21	4.52
E	-3846.71	-1499.60	-2305.22	-619.51	-230.73	-364.17	8.89	3.50	5.35
A3	-3755.12	-1411.39	-2266.35	-694.89	-34.30	-275.27	8.38	3.77	5.46
A4	-3571.95	-1234.96	-2284.29	-1115.47	593.60	-173.79	6.66	4.96	5.72
A5	-3297.18	-970.33	-2248.58	-1429.59	1514.72	-102.74	4.98	6.63	5.72
A6	-3022.42	-705.69	-2204.91	-1643.84	2593.89	-148.47	3.62	8.66	5.40
A7	-1648.59	617.48	-1060.14	-621.18	5224.71	896.88	2.50	11.21	4.76
A8	-1099.06	1146.75	-716.51	-442.33	7371.38	888.66	1.55	14.72	3.79
A9	-366.35	1852.44	-182.13	-49.98	10935.28	862.12	0.72	20.69	2.38

Table 3: Value of partial and integral excess Gibbs free energy(g^E), enthalpy(h^E) and entropy(s^E) of BI-βN system

Alloy	g_{BI}^{-E} J/mol	$g_{\beta N}^{-E}$ J/mol	g^E J/mol	h_{BI}^{-E} J/mol	$h_{\beta N}^{-E}$ J/mol	h^E J/mol	s_{BI}^{-E} J/mol/K	$s_{\beta N}^{-E}$ J/mol/K	s^E J/mol/K
A1	4331.00	150.52	651.72	85548.24	-3068.03	7556.18	207.72	-8.23	17.66
A2	1180.86	-187.85	131.64	16894.38	-6132.09	-757.02	42.01	-15.89	-2.38
E	-619.51	-230.73	-364.17	75281.73	32532.37	47205.66	209.09	90.26	131.05
A3	-694.89	-34.30	-275.27	25075.85	8645.74	14639.21	70.60	23.78	40.86
A4	-1115.47	593.60	-173.79	17347.95	13308.41	15122.21	50.04	34.46	41.45
A5	-1429.59	1514.72	-102.74	11453.81	21405.66	15938.61	34.36	53.04	42.78
A6	-1643.84	2593.89	-148.47	-6296.34	8483.14	-1081.10	-12.21	15.46	-2.45
A7	-621.18	5224.71	896.88	-10984.85	9531.15	-5657.26	-25.22	10.48	-15.95
A8	-442.33	7371.38	888.66	69182.13	419150.71	128795.78	164.60	973.47	302.38
A9	-49.98	10935.28	862.12	-7190.02	129152.00	4130.46	-16.26	269.29	7.44

Green Chemistry & Technology Letters
eISSN: 2455-3611, Vol 4, No 2, 2018, pp 01-09
https://doi.org/10.18510/gctl.2018.421

Table 4: Value of volume free energy change (ΔG_v) for BI-βN system of different undercoolings (ΔT)

Alloy	ΔG_v(J/cm^3)					
	1.0	1.5	2.0	2.5	3.0	3.5
A1	0.40	0.59	0.79	0.99	1.19	1.38
A2	0.43	0.65	0.86	1.08	1.29	1.51
E	0.46	0.69	0.92	1.15	1.38	1.62
A3	0.46	0.69	0.93	1.16	1.39	1.62
A4	0.47	0.71	0.94	1.18	1.42	1.65
A5	0.48	0.72	0.96	1.20	1.44	1.68
A6	0.49	0.74	0.98	1.23	1.47	1.72
A7	0.47	0.71	0.94	1.18	1.41	1.65
A8	0.47	0.71	0.95	1.18	1.42	1.66
A9	0.47	0.71	0.94	1.18	1.41	1.65
BI	0.48	0.72	0.95	1.19	1.43	1.67
βN	0.37	0.56	0.75	0.93	1.12	1.31

Table 5: Critical size of nucleus (r*) at different undercoolings (ΔT)

Alloy	r*(nm)					
	1.0	1.5	2.0	2.5	3.0	3.5
A1	148.82	99.21	74.41	59.53	49.61	42.52
A2	141.31	94.21	70.66	56.53	47.10	40.38
E	136.17	90.78	68.08	54.47	45.39	38.90
A3	136.72	91.15	68.36	54.69	45.57	39.06
A4	137.43	91.62	68.72	54.97	45.81	39.27
A5	138.71	92.47	69.35	55.48	46.24	39.63
A6	139.96	93.31	69.98	55.98	46.65	39.99
A7	149.98	99.98	74.99	59.99	49.99	42.85
A8	153.35	102.2	76.67	61.34	51.12	43.81
A9	158.12	105.4	79.06	63.25	52.71	45.18
BI	159.98	106.7	79.99	63.99	53.33	45.71
βN	152.25	101.5	76.13	60.90	50.75	43.50

Table 6: Value of ΔG^* for binary product of BI-βN system at different undercooling (ΔT)

Alloy	$\Delta G^* \times 10^{16}$ (J)					
	1.0	1.5	2.0	2.5	3.0	3.5
A1	27.32	12.14	6.83	4.37	3.04	2.23
A2	25.46	11.32	6.37	4.07	2.83	2.08
E	24.41	10.85	6.10	3.91	2.71	1.99
A3	24.77	11.01	6.19	3.96	2.75	2.02
A4	25.65	11.40	6.41	4.10	2.85	2.09
A5	26.91	11.96	6.73	4.31	2.99	2.20
A6	28.20	12.53	7.05	4.51	3.13	2.30
A7	33.28	14.79	8.32	5.33	3.70	2.72
A8	35.73	15.88	8.93	5.72	3.97	2.92
A9	38.98	17.32	9.75	6.24	4.33	3.18
BI	40.91	18.18	10.23	6.54	4.55	3.34
βN	27.60	12.27	6.90	4.42	3.07	2.25